Modeling Underwater Light Transmission: Turbidity Effect

Summary and Literature Review

Oluwaferanmi Agbolade, Gowri Sunkara, Tasnim Mim
Department of Mathematics, Louisiana State University
Advisors: Dr. Nadejda Drenska

Abstract

Underwater optical communication links promise high bandwidth, low latency, and phase-sensitive modulation. We model same-depth laser links using Beer–Lambert attenuation with Jerlov-type diffuse attenuation coefficients to establish a baseline channel transmittance, and we augment it with a stochastic turbidity model to capture heterogeneity. This summary consolidates the theoretical foundations, methods, and results from our poster and extends with a focused literature review of CV-QKD in ocean channels, Jerlov classification schemes, and measured IOPs for water types.

1 Introduction

Underwater wireless optical communication (UWOC) performance is governed by absorption, scattering, and turbidity. For a path length d and wavelength λ, Beer–Lambert attenuation gives

$$T(d, \lambda) = \exp\big(- K_d(\lambda)\, d\big),$$

where $K_d(\lambda)$ is the diffuse attenuation coefficient. We use Jerlov water-type representative $K_d(\lambda)$ spectra to anchor a physically grounded baseline for channel transmittance, which

is directly useful for communication and CV-QKD link budgets. Jerlov's taxonomy (I, IA, IB, II, III; 1C–9C) classifies waters by spectral optical clarity and is commonly expressed via transmittance through 1 m and depth-averaged K_d over 0–10 m.

2 Theory and modeling

2.1 Beer–Lambert baseline

- **Deterministic model:** For each Jerlov type and $\lambda \in [450, 550]$ nm (20 nm steps), compute $T_c(d, \lambda) = \exp(-K_d(\lambda)d)$ vs. distance d. Clear waters exhibit slower decay than turbid coastal types.

- **Absorption vs. scattering:** Both contribute to $K_d(\lambda)$ but impact coherence differently. Absorbing constituents (e.g., phytoplankton pigments) and scattering particles (e.g., mineral NAP, microbubbles) change spectral shape and path loss; classification schemes distinguish Case 1 (phytoplankton-dominated, co-varying CDOM/detritus) from Case 2 (non-covarying inorganic/terrigeneous constituents).

2.2 Stochastic turbidity

- **Heterogeneity model:** The normalized received intensity

$$X = \frac{I}{I_0} \sim \mathcal{N}(\mu, \sigma^2), \quad \mu = \exp(-K_d d), \quad \sigma = \eta\,\mu,$$

truncated to $X \in [0, 1]$, where η (scaled by cells/m) parameterizes heterogeneity. This yields PDFs and histograms that quantify variability at fixed d, λ.

2.3 Numerical implementation

- Compute $T_c(d, \lambda)$ for representative Jerlov types, then sample X via Monte Carlo to visualize PDFs across distances and heterogeneity levels. Aggregate means to produce heatmaps

of mean transmittance.

3 Literature review

3.1 Jerlov classification and optical taxonomies

Jerlov water types are defined by spectral transmittance and diffuse attenuation and remain a foundational classification used to contextualize ocean color and penetration depth. The Ocean Optics Web Book reviews classification schemes, including Jerlov's AOP-based types and the Case 1/Case 2 distinction, noting that natural waters form a continuum and the binary split can be misleading when absorption and scattering drivers decouple. Morel (1988) provides approximate links between Jerlov open-ocean types and chlorophyll, and subsequent work relates Jerlov types to consistent IOP sets that reproduce K_d spectra numerically.

3.2 Measured IOPs for Jerlov water types

Measured and synthesized IOP tables (absorption/scattering coefficients across wavelength) provide a consistent basis to generate $K_d(\lambda)$ spectra matching Jerlov types. The Optica article's table of measured IOPs for Jerlov water types offers parameter sets that, when used in radiative transfer, yield K_d consistent with Jerlov's AOP classification, supporting physics-based mapping from composition to expected attenuation.

3.3 CV-QKD in ocean channels

Meena and Banerjee (2024) develop a CV-QKD framework for underwater channels with a turbulence model using ABCD matrix cascades through discrete cells of varying refractive index and curvature. The work analyzes attenuation versus depth (450–550 nm window), turbulence-induced spreading/fading, and protocol-level enhancements via non-Gaussian postselection and virtual photon subtraction. They report: - Contour maps of received

intensity broadening with distance under turbulence. - PDFs of I/I_0 showing dispersion changes with distance and turbulence cell density. - Transmittance T_c vs. distance for different ocean profiles and geometries (same vs. different depth). - Key-rate comparisons (Gaussian vs. non-Gaussian) under attenuation-only and combined attenuation+turbulence, with reverse reconciliation and excess noise parameters as controls.

This complements our Beer–Lambert baseline by incorporating beam-propagation physics in turbulence and linking channel parameters to CV-QKD performance (mutual information, Holevo bound) through covariance-matrix analyses. Their emphasis on the blue–green window (450–550 nm) and depth-dependent attenuation aligns with Jerlov guidance and ocean-optics understanding.

4 Results placeholders

Deterministic transmittance vs. distance (Beer–Lambert)

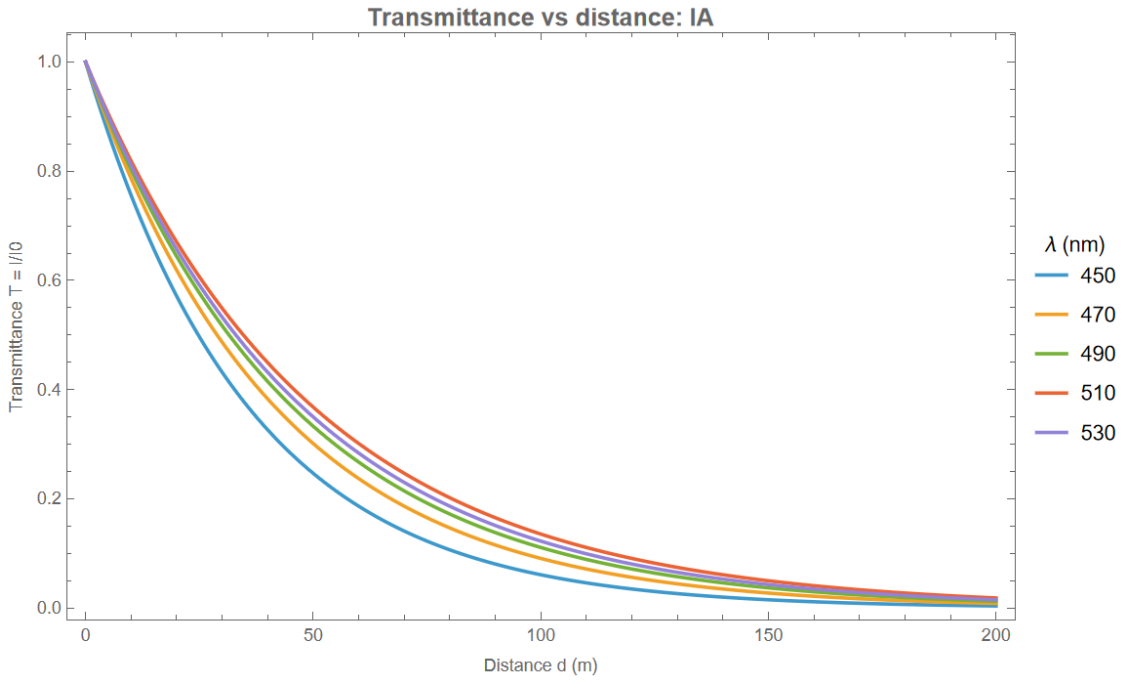

Figure 1: Transmittance $T_c(d, \lambda)$ vs. distance for selected Jerlov types and wavelengths (450–550 nm).

Monte Carlo PDFs of normalized intensity

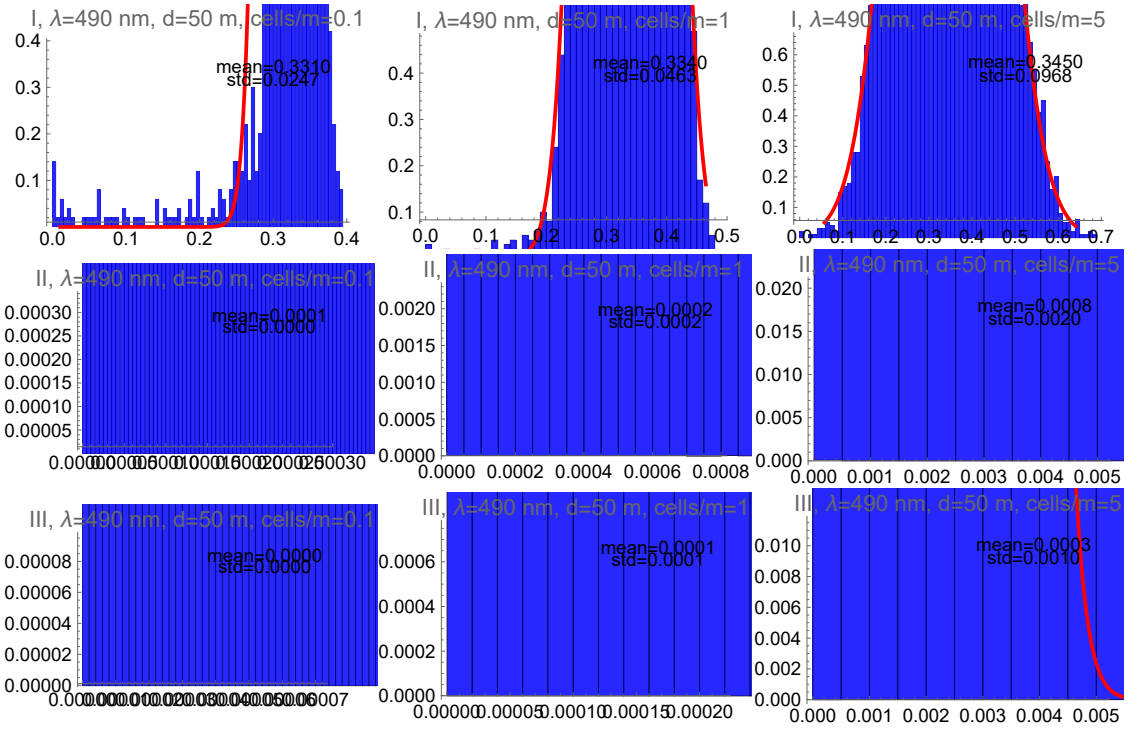

Figure 2: PDFs of $X = I/I_0$ across distances and heterogeneity (cells/m), truncated to $[0, 1]$.

Mean transmittance heatmaps

5 Discussion

- The Beer–Lambert + Jerlov framework provides a transparent, reproducible baseline for underwater channel loss and is suitable for systems analysis and CV-QKD key-rate estimates. - Stochastic turbidity modeling captures small-scale heterogeneity, enabling uncertainty visualization around deterministic expectations. - Measured/synthesized IOP tables for Jerlov types support physics-grounded parameterization, bridging composition to $K_d(\lambda)$ and transmittance. - When turbulence is material, ABCD-based beam propagation complements scalar attenuation, connecting optical design (waist/apertures) and environment (salinity, temperature) to received intensity maps and CV-QKD covariance parameters.

Figure 3: Heatmaps of mean $T_c(d, \lambda)$ across distance and wavelength for representative Jerlov types.

6 Conclusions and future work

Our approach maps water type to expected channel transmittance with uncertainty bands from turbidity, aligning with ocean-optics classification and CV-QKD needs. Next steps: - Separate absorption and scattering contributions explicitly and validate against IOP-based synthesis for chosen Jerlov types. - Integrate turbulence cells/flows (ABCD) with attenuation to produce joint transmittance and irradiance predictions usable in CV-QKD rate calculations. - Validate with field data and curated $K_d(\lambda)$ datasets; leverage classification guidance (Case 1/Case 2) to interpret spectral and spatial variability.

References

1. Ocean Optics Web Book: Classification Schemes (Inherent and Apparent Optical Properties). `https://www.oceanopticsbook.info/view/inherent-and-apparent-optical-properti`

classification-schemes

2. Measured IOPs of Jerlov water types, Optica (Applied Optics) table. https://opg.optica.org/ao/fulltext.cfm?uri=ao-61-33-9951#t004

3. N. G. Jerlov, *Marine Optics*, Elsevier (1976).

4. R. Meena, S. Banerjee, "Continuous Variable Based Quantum Communication in the Ocean," arXiv:2401.13243 (2024).

5. C. D. Mobley, *Light and Water: Radiative Transfer in Natural Waters*, Academic Press.

Table 1: Diffuse attenuation coefficients $K_d(\lambda)$ (m^{-1}) for Jerlov types IA, IB, II, III, 1C, 3C, 5C (450–550 nm).

Wavelength (nm)	IA	IB	II	III	1C	3C	5C
450	0.0264	0.0340	0.0620	0.1240	0.1790	0.3190	0.5350
460	0.0260	0.0330	0.0620	0.1100	0.1390	0.2400	0.4010
470	0.0256	0.0330	0.0580	0.1010	0.1340	0.2250	0.3820
480	0.0266	0.0320	0.0580	0.0990	0.1200	0.1970	0.3190
490	0.0291	0.0390	0.0670	0.1090	0.1200	0.1970	0.3190
500	0.0316	0.0390	0.0670	0.0990	0.1200	0.1970	0.3190
510	0.0391	0.0450	0.0730	0.1150	0.1300	0.2050	0.3300
520	0.0466	0.0520	0.0790	0.1210	0.1350	0.2100	0.3400
530	0.0534	0.0570	0.0840	0.1290	0.1400	0.2200	0.3500
540	0.0596	0.0650	0.0920	0.1380	0.1500	0.2300	0.3600
550	0.0658	0.0726	0.1000	0.1450	0.1600	0.2400	0.3700